RAPID COMMUNICATIONS

PHYSICAL REVIEW A

ATOMIC, MOLECULAR, AND OPTICAL PHYSICS

THIRD SERIES, VOLUME 48, NUMBER 6 DECEMBER 1993

RAPID COMMUNICATIONS

The Rapid Communications section is intended for the accelerated publication of important new results. Since manuscripts submitted to this section are given priority treatment both in the editorial office and in production, authors should explain in their submittal letter why the work justifies this special handling. A Rapid Communication should be no longer than 4 printed pages and must be accompanied by an abstract. Page proofs are sent to authors.

Effect of rotations on stabilization in high-intensity photodissociation of H_2^+

E. E. Aubanel, A. Conjusteau, and A. D. Bandrauk

Laboratoire de Chimie Théorique, Faculté des Sciences, Université de Sherbrooke, Sherbrooke, Québec, Canada J1K 2R1

(Received 31 March 1993)

Photodissociation probabilities of rotationless H_2^+ at $\lambda = 769$ nm, from numerical solutions of the time-dependent Schrödinger equation, exhibit minima which are attributed to trapping in one- and three-photon field-induced potential wells, leading to molecular stabilization. Rotational excitations are shown to destroy the three-photon stabilization, whereas the one-photon trapping and stabilization of the bound molecular states at high intensities can persist in the presence of rotational excitation.

PACS number(s): 33.80.Gj

Recent time-dependent numerical simulations have confirmed that molecular photodissociation produced by subpicosecond laser pulses can be suppressed as a result of stabilization of the molecule at high intensities such that electronic Rabi frequencies exceed molecular vibrational frequencies [1–4]. Such stabilization is attributed to trapping in laser-induced adiabatic potential wells arising from laser-induced avoided crossings in the time-independent dressed-molecule representation [5]. Theoretical work has up to now concentrated on trapping due to one-photon avoided crossings. Possible trapping due to a three-photon avoided crossing has been the subject of a recent experimental inquiry [6]. Observation of alignment in product angular distributions in high-intensity photodissociation of I_2 and HCl^+ [7,8] implies that sig-

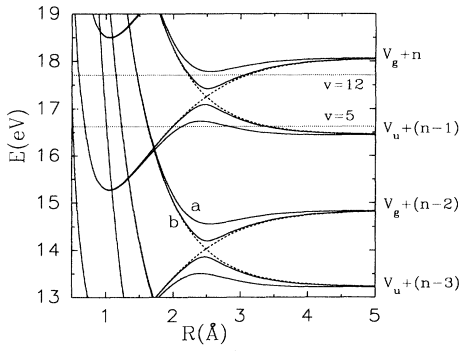

FIG. 1. Diabatic (field-free) (dashed line) and adiabatic (solid line) rotationless field-molecule potentials for H_2^+ with $\lambda = 769$ nm at intensities 10^{12} W/cm^2 (a), and 10^{13} W/cm^2 (b). Also shown are diabatic vibrational levels $v = 5, 12$.

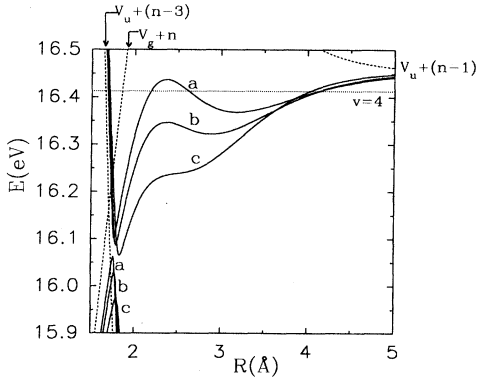

FIG. 2. Enlargement of Fig. 1 in the region of three-photon avoided crossing, at intensities 2.6×10^{13} (a), 3.3×10^{13} (b), and 4.4×10^{13} W/cm^2 (c). Also shown is the diabatic vibrational level $v = 4$.

nificant rotational excitation takes place during short intense pulses. Previous theoretical work has shown that rotational excitation can substantially alter, enhance, or destroy stabilization [1,9].

It is our purpose to examine the effect of rotational excitation on the time-dependent stabilization during photodissociation of H_2^+ at $\lambda = 769$ nm due to one- and three-photon avoided crossings. This is illustrated in Fig. 1 for photodissociation from an initial bound vibrational level in the ground $^2\Sigma_g^+$ electronic potential to a continuum (dissociative) nuclear state of the repulsive $^2\Sigma_u^+$ electronic potential. In the time-independent dressed picture, the field-molecule potential $V_g(^2\Sigma_g^+, R) + n\hbar\omega$ crosses the $V_u(^2\Sigma_u^+, R) + (n-1)\hbar\omega$ and the $V_u(^2\Sigma_u^+, R) + (n-3)\hbar\omega$ potentials, as a consequence of conservation of total energy after absorption of one and three photons, respectively. Also shown is the $V_g(R) + (n-2)\hbar\omega$ potential, which crosses the $V_u(R) + (n-3)\hbar\omega$ potential. Figure 1 shows that one can describe the molecular states either in the original unperturbed (crossing) state description called diabatic or the new field-induced states obtained by diagonalizing a potential matrix containing diabatic potentials $V_u(R) + (n + 2l + 1)\hbar\omega$ and $V_g(R) + (n + 2l)\hbar\omega$ ($l = 0, \pm1, \pm2, \ldots$) coupled by [1,5,10] :

$$V_{gu}(R) = \langle {}^2\Sigma_u^+, n \pm 1 | \mathbf{d}(R) \cdot \mathbf{E}_0/2 | {}^2\Sigma_g^+, n \rangle = \hbar\omega_R, \quad (1)$$

$$\begin{aligned} \hbar\omega_R/2\,(\mathrm{cm}^{-1}) &= 5.85 \times 10^{-4} \sqrt{I(\mathrm{W/cm}^2)}\, d(\mathrm{a.u.}) \\ &= \gamma d(\mathrm{a.u.})/2, \end{aligned} \quad (2)$$

where ω_R is the electronic Rabi frequency, $d(R)$ is the electronic dipole moment in atomic units, n is the photon number, and γ is a unit conversion factor. These radiative couplings give rise to laser-induced adiabatic potentials. We achieved converged adiabatic potentials in Figs. 1 and 2 with a potential matrix of order 12 ($l = 0, \pm1, \pm2, 3$). Note that at the higher intensity in Fig. 1 the energy gap at the one-photon crossings [between the pairs $V_g(R) + n\hbar\omega$, $V_u(R) + (n-1)\hbar\omega$ and $V_g(R) + (n-2)\hbar\omega$, $V_u(R) + (n-3)\hbar\omega$] is so large (1.0 eV) that these crossings are adiabatic, i.e., the Landau-Zener crossing probability is equal to 1 [5,10]. The adiabatic potential well formed by the one- and three-photon avoided crossings, which will support new quasi-bound nuclear states [5,10], is shown for three intensities, $I = 2.6, 3.3, 4.4 \times 10^{13}$ W/cm^2, in Fig. 2. The energy gap at the three-photon crossing, which is mediated by three-photon nonresonant processes, is much smaller than at the resonant one-photon crossing: 0.09 eV at the highest intensity. The shape of the adiabatic potential varies from a double well at the lowest intensity to a single broad well at the highest intensity due to the influence of the upper one-photon avoided crossing. Note that the well flattens asymptotically to $V_u(R) + (n-1)\hbar\omega$ for $R > 5$Å at 16.45 eV, which is just above the vibrational level $v = 4$ ($E = 16.41$ eV) of the field-free V_g potential.

In our numerical calculations we take as initial states the rotational level N=5, $J = N + 0.5$, $m_J = 0.5$ of the vibrational levels $v = 5, 12$ of H_2^+. In this case, i.e., $m_J = 0.5$, the molecule is parallel to the field, which results in maximum radiative coupling. We limit ourselves to linear polarization, i.e., $\Delta m_J = 0$. Trapping is thus expected to occur for the smallest m_J sublevels. The time-dependent Schrödinger equation for a basis of rotational states, $\chi = [\chi_J]$ is

$$\left(i\hbar\frac{\partial}{\partial t} + \frac{\hbar^2\nabla^2}{2m} \right) \chi(R,t) = \mathcal{V}\chi(R,t), \quad (3)$$

where $\mathcal{V}$ is a tridiagonal matrix with diagonal elements (for initial $J = 5.5$)

$$V_{N=2j+1}(R) = V_g(R) + V_r(R,N), \quad (4a)$$

$$V_{N=2j}(R) = V_u(R) + V_r(R,N), \quad (4b)$$

where $j = 0, 1 \ldots$,

$$V_r(R,N) = \hbar^2 N(N+1)/(2\mu R^2),$$

and off-diagonal elements

$$V_{J,J+1} = V_{gu}\left[(J + 1 + m_J)(J + 1 - m_J)\right]^{1/2}/2(J+1), \quad (5)$$

where

$$V_{gu}(R,t) = \frac{eR}{2} E_0(t)\cos(\omega t), \quad (6)$$

and $R/2$ is the electronic transition moment $\langle 1\sigma_g | r | 2p\sigma_u \rangle$ [5,11]. We note that such diverging transition moments are typical of symmetric molecular ions and create unusually large nonperturbative radiative couplings. We have neglected diagonal coupling terms $V_{J,J}$, which is valid for large J in the case of $^2\Sigma$-$^2\Sigma$ transitions [9]. Two types of two-state calculations were performed as well: one using two coupled time-dependent Schrödinger equations with rotationless potentials V_g,V_u,V_{gu}, and the other using a rotational matrix containing two channels corresponding

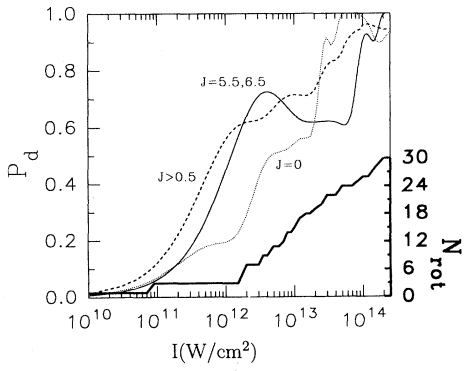

FIG. 3. Dissociation probabilities, P_d, from the initial vibrational level $v = 12$ from rotationless (dotted line), two-channel (solid line), and full rotational (dashed line) calculations with a 100-fs pulse. The last two calculations are from the initial rotational level $J = 5.5$, $m_J = 0.5$. Also shown is N_{rot}, the number of rotational levels excited to 90% of total probability.

to $V_g + V_r(5)$ and $V_u + V_r(6)$ ($m_J = 0.5$).

The discretized nuclear wave function χ was propagated in time [Eq. (3)] using the second-order split-operator method [12–14]. Propagation was continued past the end of the pulse to allow all of the continuum functions to dissociate, i.e., pass $R = 5$ Å. We then obtained the dissociation probability P_d by integrating the density $|\chi \cdot \chi|$ from $R = 5$ Å to the end of the grid. The pulse line shape used was

$$E_0(t) = \gamma c_1\{\mathrm{sech}[a_0(t - t_0)/t_0] - c_0\}, \qquad (7)$$

for $0 \leq t \leq 2t_0$, $E_0(t) = 0$ otherwise, where $c_0 = \mathrm{sech}(a_0)$, $c_1 = 1/(1 - c_0)$, and $a_0 = 2$.

One-photon trapping. The dissociation probability P_d, as a function of intensity, from initial rotational level $J = 5.5$, $m_J = 0.5$, of vibrational level $v = 12$, after a 100-fs pulse, is shown in Fig. 3, from full rotational (dashed line), two-channel (solid line), and rotationless (dotted line) calculations. At low intensity, for the full and two-channel rotational results, $P_d \propto I$, signifying perturbative one-photon absorption, followed by extrema and plateaux characteristic of nuclear trapping [1,2,5]. The rotationless curve has a different shape below 10^{13} W/cm^2 than the two-channel curve, which is due to laser-induced diabatic-adiabatic coincidences [1,2,5], i.e., there is trapping at low ($\sim 10^{12}$ W/cm^2) intensity in the former case only; otherwise the two curves are offset by a factor of 4, because $V_{5.5,6.5} \simeq 0.5V_{gu}$ [Eq. (5)]. The behavior of P_d as a function of time at intensities corresponding to minima in the solid curve in Fig. 3 is similar to the behavior of one-photon trapping at 212.8 nm, Fig. 3 of [2], and is therefore not shown here.

The full rotational curve in Fig. 3 has features similar to the two-channel curve, but shifted downward in intensity. This shifting is due to each rotational state being coupled to two others in the former case, but only to one other in the latter case [9]. The number of rotational states, N_{rot}, which were populated (to 90% of the total probability) by the end of the pulse, i.e., the spread of N [Eq. (4)], is shown as a function of intensity in Fig. 3. Note that excitation rises rapidly as stabilization begins to take place, for $I > 10^{12}$ W/cm^2, and reaches 30 rotational levels by 2.5×10^{14} W/cm^2. This suggests that

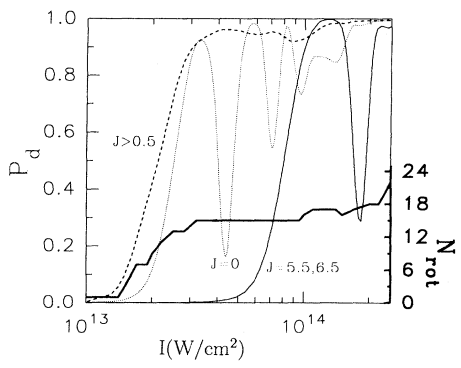

FIG. 4. Same as Fig. 3, except for the initial vibrational level $v = 5$, and for the 300-fs pulse.

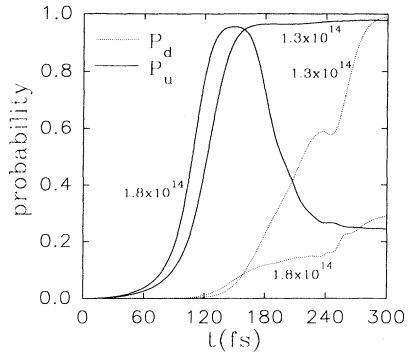

FIG. 5. Dissociation probability (P_d, dotted line) and probability of occupying the $^2\Sigma_u^+$ level (P_u, solid line) as a function of time, from two-channel calculation with 300-fs pulse, from the initial level $J = 5.5$, $m_J = 0.5$, $v = 5$, at 1.3×10^{14} and 1.8×10^{14} W/cm^2.

trapping of the nuclei permits longer interaction with the field and therefore increased rotational excitation, leading thereby to alignment as observed by Corkum and co-workers [7,8]. This excitation, however, destabilizes the trapping, which shows up as the step features in the full rotational curve. Therefore, it can be concluded that rotational excitation diminishes the stabilization of dissociation present in rotationless results, but that the trapping of the nuclei manifests itself as increased rotational excitation.

Three-photon trapping. Dissociation probabilities, P_d, and rotational excitation, N_{rot}, from the $J = 5.5$, $m_J = 0.5$, $v = 5$ level, after a 300-fs pulse, are shown in Fig. 4, in the same format as Fig. 3. The rotationless results (dotted line) show a dependence on intensity that rises from I^5 below 1.5×10^{13} W/cm^2 up to I^7 before saturation, followed by well pronounced minima. Similar dependence of P_d on I has been studied recently, for the rotationless problem, in $H_2{}^+$ [15]. At low intensity, less than 10^{12} W/cm^2, dissociation occurs in the $V_u + (n-3)\hbar\omega$ and $V_g + (n-2)\hbar\omega$ channels (see Fig. 1), resulting in net absorption of 3 and 2 photons, respectively. At higher intensities, greater than 10^{13} W/cm^2, tunnelling into the $V_u + (n-1)\hbar\omega$ channel occurs, resulting in net absorption of one photon. At still higher intensities the three-photon crossing begins to dominate, resulting in products in the $V_g + (n-2)\hbar\omega$ channel, since its crossing with $V_u + (n-3)\hbar\omega$ is now adiabatic. The two-channel (solid line) and rotationless (dotted line) curves are of similar shape, but offset by a factor of 4. The lowest minimum in the rotationless curve is very deep, reaching $P_d \simeq 0.2$ at 3.3×10^{13} W/cm^2, and is followed by further extrema. The stabilization can be understood by considering Figs. 2 and 5. The probability of occupying the $^2\Sigma_u^+$ state, P_u, and P_d vs time is shown in Fig. 5 for the first maximum and minimum of the two-channel calculation. Thus in the first case, at 1.3×10^{14} W/cm^2 (or similarly at 3.3×10^{13} W/cm^2 in the rotationless calculation), dissociation proceeds rapidly, with all probability transferred to the $^2\Sigma_u^+$ state by 150 fs. In the second case, at 1.8×10^{14} W/cm^2 (or 4.4×10^{13} W/cm^2 in the

rotationless calculation), P_u reaches a maxiumum at 150 fs, then drops down to 0.23 by the end of the pulse. This behavior can be understood by considering Fig. 2 : the initial vibrational level $v = 5$ is Stark shifted down into the adiabatic well formed by the one- and three-photon crossings. Probability is initially transferred to the $^2\Sigma_u^+$ state after the one-photon crossing (at 2.5 Å) is passed, but then returns to the ground state as a wave packet after hitting the right turning point of the adiabatic potential and recrossing the one-photon crossing into the $^2\Sigma_g^+$ ground state. At still higher intensities ($> 4.4 \times 10^{13}$ W/cm^2 for the rotationless case), or for longer pulses, multiple oscillations in this adiabatic well can occur; this explains the further extrema in P_d vs I in Fig. 4.

As in Fig. 3 the full rotational curve is shifted downwards in intensity with respect to the two-channel curve, and two shallow minima are present. The three-photon rotational excitation $N_{\rm rot}$ as a function of intensity shows a very different behavior than in the one-photon case (Fig. 3). The initial rise of P_d is now accompanied by a rise in rotational excitation $N_{\rm rot}$. This is not surprising, since several photons are absorbed/emitted before dissociation takes place (recall $P_d \propto I^7$ above). Compare this to Fig. 3, where only one photon was involved and $N_{\rm rot}$ did not rise during the initial rise of P_d . Subsequent shallow minima are present in P_d, but are not accompanied by an increase in $N_{\rm rot}$.

We conclude therefore by emphasizing the main difference between the one-photon and three-photon high intensity photodissociation of H_2^+ which arises from the different rotational pumping for each. Thus in the one-photon case, maximum rotational excitation occurs at intensities where adiabatic trapping or stabilization occurs for the two-channel photodissociation model (solid line, Fig. 3). Since such stabilization is a nonlinear effect [5], i.e., involving multiple photon excitation, then the trapping and rotational excitation are strongly correlated, with the end result that rotational excitation destabilizes the trapping. Conversely, maximum dissociation in the two-channel model can be decreased by rotational excitation, as a result of the creation of coincidences between diabatic and adiabatic states [9] through the rotational excitation (see Fig. 3, $I = 2 \times 10^{12}$ W/cm^2).

In the three-photon photodissociation, because the excitation is of higher order, multiple rotational excitation occurs readily as the dissociation probability reaches its first maximum (Fig. 4). This immediately excludes any trapping or stabilization by laser-induced adiabatic wells (Fig. 2), the latter corresponding to a two-channel single rotational excitation model. Thus multiple rotational excitations couple an initial vibrational-rotational (v,J) level to many continua, thus enhancing dissociation.

Recently Bucksbaum and co-workers [6] have observed broad resonant features in the proton kinetic energy spectrum following photoionization of H_2^+ at 769-nm laser excitation at 10^{15} W/cm^2. They ascribe these resonance features to partial trapping of the nuclear states by three-photon adiabatic wells, illustrated here in Fig. 2, at an intensity of about 10^{14} W/cm^2. Our present results indicate that no laser-induced long lived states, i.e., sharp resonances, should exist in three-photon dissociation due to multiple rotational excitation. Three-photon dissociation at 10^{14} W/cm^2 seems to be rather complete. We have verified our calculations with other pulse shapes, and find that, in general, only one-photon resonances can be stabilized in the presence of rotational excitation. The present model involves only two electronic states, $^2\Sigma_g^+$ and $^2\Sigma_u^+$. Higher order electronic states, which also have diverging transition moments $eR/2$ (*eg.*, $2\sigma_g - 2\sigma_u$), giving rise to large molecule-radiation coupling, could conceivably also create resonance effects in the photoionization of H_2^+. This aspect has not yet been clarified.

[1] E. E. Aubanel, J. M. Gauthier, and A. D. Bandrauk, Phys. Rev. A **48**, 2145 (1993).
[2] E. E. Aubanel, A. D. Bandrauk, and P. Rancourt, Chem. Phys. Lett. **197**, 419 (1992).
[3] A. Giusti-Suzor and F. H. Mies, Phys. Rev. Lett. **68**, 3869 (1992).
[4] G. Yao and S. I. Chu, Chem. Phys. Lett. **197**, 413 (1992).
[5] A. D. Bandrauk and M. L. Sink, Chem. Phys. Lett. **57**, 569 (1978); J. Chem. Phys. **74**, 1110 (1981).
[6] A. Zavriyev, P. H. Bucksbaum, J. Squier, and F. Salin, Phys. Rev. Lett. **70**, 1077 (1993).
[7] D. T. Strickland, T. Beaudoin, P. Dietrich, and P. B. Corkum, Phys. Rev. Lett. **68**, 2755 (1992).
[8] P. Dietrich and P. B. Corkum, J. Chem. Phys. **97**, 3187 (1992).
[9] A. D. Bandrauk and G. Turcotte, J. Chem. Phys. **77**, 3867 (1982); J. Phys. Chem. **87**, 5098 (1983).
[10] A. D. Bandrauk, *Molecules in Laser Fields* (Dekker, New York, 1993).
[11] R. S. Mulliken, J. Chem. Phys. **7**, 20 (1939).
[12] R. Heather and H. Metiu, J. Chem. Phys. **86**, 5009 (1987).
[13] A. D. Bandrauk and H. Shen, Chem. Phys. Lett. **176**, 428 (1991); J. Chem. Phys. (to be published).
[14] M. D. Feit and J. A. Fleck, J. Chem. Phys. **78**, 2578 (1984).
[15] G. Jolicard and O. Atabek, Phys. Rev. A **46**, 5845 (1992).